

## Accepted Manuscript

### Electromechanical Stability of Dielectric Elastomer Composites with Enhanced Permittivity

Bo Li, Hualing Chen, Jinxiong Zhou

PII: S1359-835X(12)00347-8  
DOI: <http://dx.doi.org/10.1016/j.compositesa.2012.11.013>  
Reference: JCOMA 3299

To appear in: *Composites: Part A*

Received Date: 3 September 2012  
Revised Date: 30 October 2012  
Accepted Date: 18 November 2012



Please cite this article as: Li, B., Chen, H., Zhou, J., Electromechanical Stability of Dielectric Elastomer Composites with Enhanced Permittivity, *Composites: Part A* (2012), doi: <http://dx.doi.org/10.1016/j.compositesa.2012.11.013>

This is a PDF file of an unedited manuscript that has been accepted for publication. As a service to our customers we are providing this early version of the manuscript. The manuscript will undergo copyediting, typesetting, and review of the resulting proof before it is published in its final form. Please note that during the production process errors may be discovered which could affect the content, and all legal disclaimers that apply to the journal pertain.

# Electromechanical Stability of Dielectric Elastomer Composites with Enhanced Permittivity

Bo Li <sup>a,b</sup>, Hualing Chen <sup>a,b (\*)</sup>, Jinxiong Zhou <sup>a,c</sup>

*a. State Key Laboratory for Strength and Vibration of Mechanical Structures, Xi'an Jiaotong University, Xi'an, 710049, P. R. China*

*b. School of Mechanical Engineering, Xi'an Jiaotong University, Xi'an, 710049, P. R. China*

*c. School of Aerospace, Xi'an Jiaotong University, Xi'an, 710049, P. R. China*

(\*) Corresponding author E-mail: hlchen@mail.xjtu.edu.cn  
Tel/Fax: +86-29-82660487

**Abstract**

Dielectric elastomers when doped with high permittivity fillers, such as ceramic particles, achieve enhanced dielectric properties, which lower the voltage required for actuation. A thermodynamic model is proposed which investigates the electromechanical deformation and stability in these dielectric elastomer composites. The process of electromechanical coupling is analyzed with particular emphasis on the saturated polarization of the ceramic fillers, which modifies the instability due to electrostriction. The stability characteristics are studied using established principles, and provide information for achieving the goal of high performance stretchable dielectric actuators.

**Keywords**

- A. Material: Ceramic-matrix composites; Smart material
- B. Property: Physical properties; Mechanical properties
- C. Analysis: Analytical modeling

## 1. Introduction

Electro-active polymers (EAPs) are soft active materials, which are capable of responding with mechanical deformation or movement when subject to electrical stimulation. Differing from conventional smart materials, e.g. piezoelectric ceramic or shape memory alloys, EAPs feature elasticity, flexibility, and a fast response. Among various EAPs, the dielectric elastomer, which is categorized as an electric-field-EAP, expands well, in excess of 100% when exposed to an external electric field [1].

The dielectric elastomer is an elastic dielectric. When sandwiched between two compliant electrodes and subjected to a voltage, the dielectric elastomer membrane reduces in thickness and expands in area, due to Maxwell stress [2]. A unique feature of dielectric elastomers is the ability to expand up to 500% of their original area within 1 ms [3]. This electromechanical deformation has attracted extensive attention in the last decade and has been studied in diverse applications, including soft robots, adaptive optics, Braille displays, and electric generators [4-8].

Dielectric elastomers are susceptible to modes of instability during electromechanical deformation. Upon a voltage, the dielectric membrane deforms until a stable state that the electrostatic stress is in equilibrium with the elastic stress. When the voltage increases and exceeds a critical level, the membrane becomes thinner, so the same voltage produces a higher electric field which further squeezes the membrane that the elastic stress fails in equilibrium until electrical breakdown. In previous investigation, this failure mode was named pull-in instability or electromechanical instability. Zhao and Suo proposed a thermodynamics method to

determine the conditions that the stable deformation was attained only if the free energy form of the dielectric elastomer was positive defined [9]. They also predicted the critical values of voltage and stretch at the onset of instability, which agreed well with experiments. Pull-in has been recognized as the key issue that hinders large-scale stable deformation in dielectric elastomer. After the pull-in instability, however, the elastomer may survive without electrical breakdown; and it attains a much smaller thickness without a continuous deformation, due to snap-through instability [7]. This behavior is understood by considering the elastomer under tension (Fig. 1a). On approaching the extension limit of polymer chains,  $\lambda_{im}$ , the elastomer stiffens sharply. When the deformation is caused by a voltage rather than mechanical forces, the voltage-stretch curve may take the form shown in Fig. 1b. The voltage attains a local peak value at stretch  $\lambda_c$ , corresponding to the onset of the pull-in instability. As the voltage ramps up further, the membrane snaps and is stabilized at a stretch close to  $\lambda_{im}$ . Due to the instabilities of the dielectric elastomer, the maximum deformation of actuation in equal-biaxial stretch is limited below  $\lambda_c=1.26$  [4, 10].

In addition to the two modes of instability, high voltages (>3000 V) are used and can be a major safety issue. Therefore, reducing the driving voltage would provide significant advances and would increase the potential applications of these materials.

Recalling the definition of Maxell stress [7]:  $p = \epsilon(\Phi/H)^2$ , where  $\epsilon$  is the permittivity of the polymer,  $\Phi$  is the voltage and  $H$  is the original thickness of the dielectric elastomer membrane: to reduce the voltage but preserve the same level of stress, one can either reduce the thickness of the film or employ a dielectric elastomer

with enhanced permittivity. Pre-stretching has been applied to reduce the membrane's thickness prior to electrical voltage activation, as documented previously [3, 4, 7-10]. Alternatively, the permittivity has been enhanced by doping high permittivity fillers into the polymeric host [11-16]. As a result, the overall permittivity is improved by 30% at least and one study observed that the instabilities described above have been suppressed [2, 14]. Besides, the reported dielectric elastomer composites benefit little hysteresis, long fatigue life (100000 cycles), and robust response [11], compared to the neat elastomer from 3M company.

Models are expected to give prediction and explanation on the coupled performance of dielectric elastomer composites. Efforts have been devoted to the laminar dielectric composites, concerning the coupling between the layers, which are not fully applicable to particle-amorphous polymer mixture [23, 24]. Previously, a theoretical model, based on experimental data of barium titanium oxide ( $\text{BaTiO}_3$ ) powder reinforced silicone elastomer, was proposed to investigate the deformation of composites, and discussed the stabilization during electromechanical coupling [14]. However, due to the differences in the physical properties of the polymeric host and reinforcement, i.e. polarization behavior, the mechanism of electromechanical stabilization differs significantly from that of a neat dielectric elastomer. To date, little appropriate fundamental interpretation, or systematic model have been established for these composites. Therefore, in this study we extend our previous discussion [14] and focus on the increased stability attributed to the high permittivity particle filler.

## 2. Equations of state

### 2.1 Free energy model in thermodynamic equilibrium

Figure 2a shows a schematic representation of a dielectric elastomer with ceramic particle additives. In this study, we idealize the mechanical and electrical properties of the composites. Filler particles may have different shapes: spherical, platelet-like, or fibrous. Most ceramics reinforcement in the experiments of dielectric elastomer composites are sphere, as confirmed in SEM micrographs [12, 33]. Therefore, in developing the theory, we first idealize the shape of ceramic inclusions are spherical. Besides, we assume that the amount of additives is sufficiently small, so that the mechanical behavior of the mixture is still preserved as hyper-elastic. We also assume that the particle reinforcements are uniformly and discretely distributed within the polymeric matrix in the direction of the applied electric field, without local charge concentrations during polarization. Furthermore, as we focus on the physical nature of the electromechanical deformation, we assume that the chemical reaction at the polymer/ceramic interface is negligible.

In the reference state (Fig. 2b) there are no forces or voltages acting on the dielectric, which has dimensions  $L_1$ ,  $L_2$ , and  $L_3$ . In the current state, when the dielectric is subjected to forces  $P_1$ ,  $P_2$ , and  $P_3$ , and to a voltage  $\Phi$ , the dielectric's dimensions change to  $l_1$ ,  $l_2$ , and  $l_3$ . The two electrodes accumulate electric charges  $\pm Q$ , and the Helmholtz free energy of the membrane is  $F$ .

When the dimensions of the dielectric change by  $\delta l_1$ ,  $\delta l_2$ , and  $\delta l_3$ , the forces do work  $P_1 \delta l_1 + P_2 \delta l_2 + P_3 \delta l_3$ . When a small quantity of charge  $\delta Q$  flows through the

conducting wire, the voltage does the work  $\Phi \delta Q$ . In equilibrium, the work done by the forces and voltage equals the increase in the free energy of the dielectric composite, as represented by Equation (1):

$$\delta F = P_1 \delta l_1 + P_2 \delta l_2 + P_3 \delta l_3 + \Phi \delta Q. \quad (1)$$

We define the density of the Helmholtz free energy by  $W = F/(L_1 L_2 L_3)$ , stretches by  $\lambda_1 = l_1/L_1$ ,  $\lambda_2 = l_2/L_2$ , and  $\lambda_3 = l_3/L_3$ , stresses by  $c_1 = P_1/(l_2 l_3)$ ,  $c_2 = P_2/(l_1 l_3)$ , and  $c_3 = P_3/(l_1 l_2)$ , the electric field by  $E = \Phi/l_3$ , and electric displacement by  $D = Q/(l_1 l_2)$ . The charge relates to the electric displacement by  $Q = D l_1 l_2$ , so that the variation of the charge is

$$\delta Q = D l_2 \delta l_1 + D l_1 \delta l_2 + l_1 l_2 \delta D. \quad (2)$$

## 2.2 Incompressible dielectric elastomer composite

When an elastomer undergoes large deformations, the change in shape is typically much larger than the change in volume. The elastomer composite which is doped with incompressible additives, is ideally taken to be incompressible as well—that is, the volume of the material remains unchanged during deformation,

$l_1 l_2 l_3 = L_1 L_2 L_3$ , so that

$$\lambda_1 \lambda_2 \lambda_3 = 1. \quad (3)$$

This assumption of incompressibility places a constraint on the three stretching directions. We regard  $\lambda_1$  and  $\lambda_2$  as independent variables, so that  $\lambda_3 = \lambda_1^{-1} \lambda_2^{-1}$ , and  $\delta \lambda_3 = -\lambda_1^{-2} \lambda_2^{-1} \delta \lambda_1 - \lambda_1^{-1} \lambda_2^{-2} \delta \lambda_2$ . Dividing both sides of Equation (1) by the volume of the membrane,  $L_1 L_2 L_3$ , and using Equations (2) and (3), we obtain



$$\delta W = (\sigma_1 - \sigma_3 + DE)\lambda_1^{-1}\delta\lambda_1 + (\sigma_2 - \sigma_3 + DE)\lambda_2^{-1}\delta\lambda_2 + E\delta D. \quad (4)$$

For an incompressible dielectric, the condition of equilibrium given by Equation (4) holds for arbitrary and independent variations of  $\delta\lambda_1$ ,  $\delta\lambda_2$ , and  $\delta D$ .

We express the electric field as a function of electric charge displacement in the dielectric

$$E = f(D). \quad (5)$$

Holding  $\lambda_1$  and  $\lambda_2$  fixed, and integrating Equation (4) with respect to  $D$ , we obtain

$$W = W_s(\lambda_1, \lambda_2) + \int_0^D f(D)dD. \quad (6)$$

The constant of integration,  $W_s(\lambda_1, \lambda_2)$ , is the free energy associated with the stretching of the elastomer in the composite. Inserting Equation (6) into Equation (4), and recalling that  $\delta\lambda_1$ ,  $\delta\lambda_2$  and  $\delta D$  are independent variations, we obtain

$$\sigma_1 - \sigma_3 = \lambda_1 \frac{\partial W_s(\lambda_1, \lambda_2)}{\partial \lambda_1} - ED, \quad (7)$$

$$\sigma_2 - \sigma_3 = \lambda_2 \frac{\partial W_s(\lambda_1, \lambda_2)}{\partial \lambda_2} - ED. \quad (8)$$

Equations (3), (5), (7) and (8) constitute the equations of state for the dielectric elastomer composites, provided the functions  $f(D)$  and  $W_s(\lambda_1, \lambda_2)$  are given.

### 3. Polarization saturation and extension limit

For ceramic-polymer composites, the overall polarization is attributed to three origins: polarization of the ceramic, polarization of the polymer, and the interfacial polarization. The interfacial polarization may have a remarkable effect on the overall polarization in some dielectric composites, especially when the concentration of the

filler is high, e.g. 40% of volume percentage. In the current research, to preserve the hyper-elasticity of the composites, the amount of filler should be controlled within a maximum level, as suggested in the experiments [11, 12]. Therefore, we limit the amount of ceramic particles of 5% in volume proportion. Due to the low concentration, these ceramic particles are mainly distributed with a large distance between each other, and consequently the interfacial effect between ceramics is weak. Meanwhile, the interfacial area between the ceramic and polymer is relatively small, compared to the laminar composites, which also suggests a weakened interfacial polarization. In the experimental report, the diameter of the ceramic particle is approximately 50 microns [12]. Within that dimension scales, the interfacial effect is less remarkable as well. The listed considerations have also been concluded in a review report, with detailed supporting information [32]. Based on these conditions, in the present context, we temporarily ignore the interfacial polarization and involve the polarizations in the two components respectively.

The polarization behaviors of the dielectric elastomer composites, under linear and saturation polarizations are shown in Fig. 3. In the dielectric elastomer/ceramic composites, both the polymer and ceramic rotational dipoles contribute to the overall polarization. In the presence of an electric field, the elastomer is linearly polarized [7], while the high permittivity dielectric fillers, i.e. BaTiO<sub>3</sub>, approach a saturated state, in which all dipoles are perfectly orientated [17-19]. The gray areas in Fig. 3 represent the electrostatic energy in the polarization process which is converted into elastic energy, in the form of mechanical deformation. By mixing the two types of dielectric,

the permittivity of the material increases, which consequently lowers the activation voltage. Additionally, due to the significant differences in the polarization behavior of the two dielectrics, the overall electromechanical coupling in the composite is modified, according to the specific material properties.

We next decompose the polarization into contributions from the dielectric elastomer and polar additives. An elastomer is a three-dimensional network of long and flexible polymers, held together by cross-links. Each polymer chain consists of a large number of monomers. The cross-links have a negligible effect on the polarization of the monomers, enabling the elastomer to polarize nearly as freely as a liquid polymer. Hence, we employ the ideal dielectric elastomer polarization function to our model, in which  $E$  is linear to  $D_m$  as [20, 21]

$$D_m = \epsilon_m E, \quad (9)$$

where  $\epsilon$  is the permittivity,  $D$  is the electric displacement, and the subscript  $m$  stands for polymeric host. Unlike linear dielectric behavior, polar dielectric reinforcements are distributed discretely inside the polymer matrix, and each of the particles may be polarized in a saturated state, where all the molecular dipoles are aligned perfectly along the direction of the electric field. Thus its specific dielectric behavior is taken to be [17, 18]

$$D_f = D_s \tanh(\epsilon_f E / D_s), \quad (10)$$

where  $f$  stands for fillers, and  $D_s$  is the saturated electric displacement of additives.

Taking the total electric displacement as the combination of the two independent origins via the volume proportion of the fillers  $\phi$ , we obtain

$$D = (1 - \phi) D_m + \phi D_f = (1 - \phi) \epsilon_m E + \phi D_s \tanh(\epsilon_f E / D_s). \quad (11)$$

Note that in this context, we apply the voltage only in one direction of the material (cf. configuration in Fig. 2). Thus, we focus on the idealized isotropic behavior in the thickness direction during the polarization, since the homogeneous distribution of fillers in the matrix has been verified in experimental characterization [13, 16]. In heterogeneous dielectric composite materials, the local electric field or charge concentrations are affected by the distribution of ceramic particles, which further influences the performance of the dielectric composite [22]. Other detailed studies have been reported in the literature [23, 24].

For evaluating the free energy due to elastomer stretching,  $W_s(\lambda_1, \lambda_2)$ , we assume that the elastomer's hyper-elasticity is unaffected by the addition of small amounts of filler. To account for the extension limit of the elastomer, we adopt the Gent model [25]

$$W_s = -\frac{\mu_c J_{\text{lim}}}{2} \log \left( 1 - \frac{\lambda_1^2 + \lambda_2^2 + \lambda_3^2 - 3}{J_{\text{lim}}} \right), \quad (12)$$

where  $\mu_c$  is the effective shear modulus of the composite, and  $J_{\text{lim}}$  is a constant characterizing the extension limit. The stretches are restricted as  $0 \leq (\lambda_1^2 + \lambda_2^2 + \lambda_3^2 - 3) / J_{\text{lim}} < 1$ . When  $(\lambda_1^2 + \lambda_2^2 + \lambda_3^2 - 3) / J_{\text{lim}} \rightarrow 0$ , the Gent model recovers the neo-Hookean model,  $W_s = (\mu / 2)(\lambda_1^2 + \lambda_2^2 + \lambda_3^2 - 3)$ . When  $(\lambda_1^2 + \lambda_2^2 + \lambda_3^2 - 3) / J_{\text{lim}} \rightarrow 1$ , the free energy represented by Equation (12) diverges, and the elastomer approaches the extension limit. For particle reinforced polymer composites, the shear modulus is derived from a group of mixing rules. To account for the effect of rigid fillers inside the soft matrices of the host, thus we express the

effective shear modulus as a function of the shear modulus of the two dielectric components [26]

$$\mu_c = \mu_m + \frac{\phi \mu_m (\mu_f - \mu_m)}{\mu_m + \beta (1 - \phi) (\mu_f - \mu_m)}, \quad (13)$$

where  $\beta$  relates to the Poisson ratio of the polymer  $\nu_m$  as  $\beta = (2(4 - 5\nu_m)) / (15(1 - \nu_m))$ . For an incompressible dielectric elastomer,  $\beta$  is reduced to 0.4.

#### 4. Electromechanical deformation and stability

By applying the model to study a membrane of dielectric elastomer composites subject to fixed equal-biaxial forces,  $P_1 = P_2 = P$  and  $P_3 = 0$ , as well as voltage  $\Phi$ , we obtain the three stretches  $\lambda_1 = \lambda_2 = \lambda$  and  $\lambda_3 = \lambda^{-2}$ . Combining Equations (9)–(13) and the special cases in Equations (7) and (8), we have

$$\frac{P}{\mu_m L_2 L_3} = \left( \frac{1 + \phi(\mu_f / \mu_m - 1)}{1 + 0.4(1 - \phi)(\mu_f / \mu_m - 1)} \right) \left[ \frac{\lambda - \lambda^{-5}}{1 - (2\lambda^2 + \lambda^{-4} - 3) / J_{\text{lim}}} - \left( \frac{(1 - \phi)\lambda^3 \frac{\epsilon_m}{\mu_m} \left( \frac{\Phi}{L_3} \right)^2 + \phi \frac{D_s \lambda \Phi}{\mu_m L_3} \tanh \left( \frac{\epsilon_f \lambda^2 \Phi \epsilon_m}{\epsilon_m D_s L_3} \right)} \right) \right]. \quad (14)$$

In plotting this equation, we normalize the voltage as  $\Phi / (L_3 \sqrt{\mu_m / \epsilon_m})$ , and the force as  $P / (\mu_m L_2 L_3)$ . The extension limit of the network is represented by the dimensionless parameter  $J_{\text{lim}}$ , and the polarization saturation of the polar dielectric component is represented by the dimensionless parameter  $D_s / \sqrt{\mu_m \epsilon_m}$ . We modify the actuation feature of the dielectric composites by regulating the amount of the additives  $\phi$ , the permittivity ratio  $\epsilon_f / \epsilon_m$ , shear modulus ratio  $\mu_f / \mu_m$ , and the saturated electric displacement  $D_s / \sqrt{\mu_m \epsilon_m}$ , as indicated by the experimental investigation [12, 13]. We use  $J_{\text{lim}} = 100$  and  $P = 0$  to represent a rubbery dielectric

elastomer composite in a stress-free state and investigate the effect of the above-stated parameters on the stability.

We adopt  $\phi = 0.05$ , and  $\mu_f / \mu_m = 1000$  from the reported experiments [11-13, 15, 16], to represent typical synthesized dielectric elastomer/ceramic composites. It should be noted that ideally, precise values for specific materials should be used; however with the values that we use in the proposed framework theory, the physical mechanism of the actuation and instability will not be fundamentally changed.

#### 4.1 Reduction of the activation voltage

When  $\mu_f / \mu_m = 1000$ ,  $\phi = 0.05$ , and  $D_s / \sqrt{\mu_m \epsilon_m} = 150$ , Fig. 4 shows that voltage for activation is reduced by increasing the permittivity ratio  $\epsilon_f / \epsilon_m$ . The result can be understood by inspecting Fig. 3 where permittivity is the slope of the polarization curve ( $D$  vs.  $E$ ). With increased permittivity, the polarization charge is increased under the same electric field, which results in a greater amount of electrostatic energy which can be converted into mechanical energy (as reflected in the area expansion). The electromechanical deformation is enhanced due to the higher permittivity reinforcement. Under the same level of applied voltage, composites of high permittivity fillers feature an improvement in deformation, see  $\epsilon_f / \epsilon_m = 50$  vs.  $\epsilon_f / \epsilon_m = 100$  in Fig. 4. Experiments have verified the effective reduction in driven voltages, where the higher of the permittivity in the ceramics, the more reduction was achieved [11, 34]. It is also observed in Fig. 4 that further increase in permittivity ratio, eliminates the instability, and a stable deformation, featuring a monotonic

voltage-stretch curve without a local peak, is attainable at  $\epsilon_f/\epsilon_m=1000$ . The high permittivity of the additives not only reduces the voltage, but also stabilizes the actuation. This phenomenon will be discussed in the following studies.

#### 4.2 Instability modification

During polarization saturation, a particular mode of polarization in the dielectric will markedly reduce the instability in soft dielectrics [17, 21]. Figure 5 shows the plots of the dielectric elastomer-based composites with different levels of dipole polarization in the additives, where  $\epsilon_f/\epsilon_m=100$ ,  $\phi=0.05$ , and  $\mu_f/\mu_m=1000$ , which are all within the range the of commonly accepted values for the material [11-16]. Either low or extremely high values of saturated electric displacement will induce instability, and stabilization is attained at a moderate level of saturated electric displacement.

This improvement in stability is interpreted by considering the physical mechanism of polarization saturation (Fig. 3). Dielectric ceramics saturate at a sufficiently high electric field, and under these conditions Maxwell stress, originated from linear polarization is no longer applicable. Instead, electrostriction is involved [27-29]. Upon a voltage, the ceramic particles elongate, changing their shape from sphere into ellipsoid, which is previously acknowledged as electrostriction. Electrostriction causes the composites membrane to thicken, in accommodation of the flattening due to the compressive Maxwell stress. Therefore, the actuation of dielectric elastomer composites is a trade-off of two effects: the elongation in

thickness due to electrostriction, and the in-plane flattening due to compressive Maxwell stress. The ceramic particle reinforcements contribute to the elongation through electrostrictive deformation. They function like supporting columns to prevent the membrane from thinning down or reaching snap-through instability, which consequently eliminates the non-monotonous voltage-stretch character. The polymeric matrix, however, is still able to produce a moderate deformation in the planar direction. In the experiments of BaTiO<sub>3</sub> doped silicone rubbers, the activated strain in area was 20% under 4% concentrations of ceramic fillers [14], which coincided with  $\lambda=1.5$  in equal biaxial stretch, as the deformation is limited by the material dielectric strength, rather than instability.

Figure 5 suggests that the instability would be eventually eliminated only if a moderate level of electric displacement is involved. Ceramic particle fillers with a low value of saturated electric displacement may possess insufficient electrostriction to prevail over Maxwell stress. Thus, the composite membrane will again suffer an excessive squeezing force leading to modes of instability, though the attainable deformation is improved a little, as Fig. 4 indicates. However, if the level of saturated electric displacement is significantly large, it may require a huge electric field to evoke electrostriction. As a result, the polarization behavior of the ceramic is still linear. The dielectric composite actuates as a conventional linear dielectric elastomer, where instability occurs without an up-ramping voltage. Therefore, a moderate value of permittivity with respect to the saturated electric field, where  $D_s / \sqrt{\mu_m \epsilon_m} = 150$  in Fig. 5, is desirable for a stable dielectric composite. For general dielectric



elastomers ( $\mu_m \approx 0.1 \text{ MPa}$  and  $\varepsilon_m \approx 44.35 \times 10^{-12} \text{ F/m}$  as given in ref. [3]),  $D_s$  is approximately  $0.3 \text{ C/m}^2$  in term of  $D_s / \sqrt{\mu_m \varepsilon_m} = 150$ , which is attainable in dielectric ceramics as verified in the experimental study on BaTiO3 [28].

#### 4.3 Stability criteria

To give a clear picture of the actuation changes from unstable to stable mode, we investigate the voltage-stretch dependence by taking the partial differential of  $\Phi$  with respect to  $\lambda$ , as shown in Fig. 6. The negative voltage-stretch dependence  $\partial\Phi/\partial\lambda < 0$  is located in the unstable mode of actuation at the onset of decreasing voltage associated with deformation, corresponding to the instability; while the positive dependence represents the stable actuation deformation. When  $\partial\Phi/\partial\lambda = 0$ , snap-through instability occurs. Figure 7 plots the voltage-stretch relationship for a dielectric elastomer composite. At each volume fraction, by varying the saturated electric displacement, a positive voltage-stretch relation at specific critical values of saturated electric displacement is identified, when the electromechanical stability changes by entering the region without snap-through (Fig. 6). This confirms experimental observations that dielectric elastomer composites with high dielectric constants deform in a large extension state over [11-13].

As seen in Fig. 7a, in composites with small amounts of dopant material ( $\phi = 0.01$ ), upon increasing the saturated polarization linearly from 10 to 200,  $\partial\Phi/\partial\lambda$  is always negative, indicating that the composites undergo unstable electromechanical deformations. From Figs. 7b and 7c, upon increasing the ceramic

dopant concentrations, a critical value for  $D_s/\sqrt{\mu_m\epsilon_m}$  is obtained, where the corresponding dielectric elastomer composites yield a stable deformation.

The difference in the stability behavior can be explained by considering the mechanical property of the ceramics. In the study of pure dielectric elastomer, prestretch offers stabilization to a specific polyacrylic membrane from 3M Company, VHB series tapes, because this material stiffens at a large deformation state. In the synthesis of dielectric elastomer composites, the silicone rubber is widely used as the host polymer since it is available in gel form. Silicone rubber fails to stiffen upon stretch [3]. However, with doped rigid ceramics, the overall elastic modulus is improved evidently for silicone rubber based dielectric composites. This improvement in elasticity is more significant with increased concentration of fillers. In Fig 7a, at a low level of doping, the actuation of dielectric elastomer composites is always unstable disregarding the value of saturation electric displacement. In Fig. 7d, at a high concentration of doping ceramics, the stiffness of the composites are remarkably increased, so that the stabilization is achieved without requiring electrostriction, attributed from a high level of saturated polarization. The values for  $\phi$ ,  $\epsilon_f/\epsilon_m$ ,  $\mu_f/\mu_m$ , and  $D_s/\sqrt{\mu_m\epsilon_m}$ , have to be set to ensure that dielectric elastomer composites operate in a stable domain.

Although snap-through instabilities are undesirable as dielectrics usually suffer electrical breakdown in the jump; in dielectrics with high breakdown strengths, as it snaps from the thick stretch state to a thinner state, the material deforms until its extension limit is reached. In this way, the deformation region after the snap-through

offers a larger deformation state. In a recent publication the snap-through instability of a dielectric balloon achieved significant voltage-triggered deformations, up to 1700% expansion [30]. Reversible snap-through instability offers new potentials for dielectric elastomer-based energy harvesters that undergo coupled electromechanical deformations [31]. Some dielectric elastomers doped with special high permittivity fillers yield not only enhanced dielectric constants but also the electrical breakdown strength is improved [15], indicating that dielectric elastomer composites are ideal candidates for energy conversion.

## 5. Conclusions

In summary, we investigated the electromechanical actuation of dielectric elastomer-based composites with high permittivity ceramic additives. A stabilized deformation for dielectric elastomer composites is attainable due to the electrostriction in the polarization of dielectric ceramic particles. The electrostriction in the ceramic fillers elongates the material and accommodates the squeezing Maxwell stress, which consequently eliminates the pull-in and snap-through instability. This model offers a new route towards achieving stable and continuous voltage-induced deformation in dielectric composites and serves as a guideline to achieve high-performance dielectric elastomer transducers.

## ACKNOWLEDGEMENTS

This work is supported by the National Natural Science Foundation of China

(Grant Nos. 10972174, 10872157 and 11072185). BL would like to express appreciation for the guidance given by Professor Zhigang Suo at Harvard University concerning the theories of polarization saturation.

ACCEPTED MANUSCRIPT

## References

1. Pelrine R, Kornbluh R, Pei QB, Joseph J. High-speed electrically actuated elastomers with strain greater than 100%. *Science* 2000; 287 (5454): 836-839.
2. Wissler M, Mazza E. Mechanical behavior of acrylic elastomer used in dielectric elastomer actuators. *Sens Actuators A* 2007; 134 (12): 494-504.
3. Brochu P, Pei QB. Advances in dielectric elastomers for actuators and artificial muscles. *Macromol Rapid Commun* 2010; 31 (1): 10-36.
4. Plante JS, Dubowsky S. Large-scale failure modes of dielectric elastomer actuators. *Int J Solids Structures* 2006; 43 (25-26): 7727-7751.
5. McKay T, O'Brien B, Calius E, Anderson I. An integrated, self-priming dielectric elastomer generator. *Appl Phys Lett* 2010; 97 (6): 062911-2.
6. Carpi F, Frediani G, Turco S, De Rossi D. Bioinspired tunable lens with muscle-like electroactive elastomers. *Adv Funct Mater*. 2011; 21 (21): 1-7.
7. Zhao XH, Hong W, Suo ZG. Electromechanical coexistent states and hysteresis in dielectric elastomers. *Phys Rev B* 2007; 76 (13): 134113-9.
8. Carpi F, Bauer S, DeRossi D. Stretching Dielectric Elastomer Performance. *Science* 2010; 330 (6012): 1759-1761.
9. Zhao XH, Suo ZG. Method to analyze electromechanical stability of dielectric elastomers. *Appl Phys Lett* 2007; 91 (6): 061921-4.
10. Li B, Chen HL, Qiang JH, et al. Effect of pre-stretch on the stabilization of dielectric elastomer actuation. *Phys D Appl Phys* 2011; 44 (15): 155301-9.
11. Opris DM, Molberg M, Walder C, et al. New Silicone Composites for Dielectric Elastomer Actuator Applications In Competition with Acrylic Foil. *Adv Funct Mater* 2011; 21 (18): 3531-3539.
12. Gallone G, Carpi F, DeRossi D, Levita G, Marchetti A. Dielectric constant enhancement in a silicone elastomer filler with lead magnesium niobate-lead titanate. *Mater Sci Eng C* 2007; 27 (1): 110-116.
13. Huang C, Zhang QM. Fully functionalized high-dielectric constant nanophase polymers with high electromechanical response. *Adv Mater* 2005; 17 (9): 1153-1158.
14. Liu LW, Liu YJ, Zhang Z, et al. Electromechanical stability of electro-active silicone filled with high permittivity particles undergoing large deformation. *Smart Mater Struct* 2010; 19 (11): 115025-30.
15. Molberg M, Crespy D, Rupper P, et al. High breakdown field dielectric elastomer actuator using encapsulated polyaniline as high dielectric constant filler. *Adv Funct Mater* 2010; 20 (19) 3280-3291.
16. Stoyanov, Kollosche M, Risse S, et al. Elastic block copolymer nanocomposites with controlled interfacial interactions for artificial muscles with direct voltage control. *Soft Mater* 2011; 7 (1): 194-200.
17. Li B, Liu LW, Suo ZG. Extension limit, polarization saturation and snap-through instability in dielectric elastomer. *Int J Smart Nano Mater* 2011; 2 (2): 59-69.

18. Yang W, Suo ZG. Cracking in ceramic actuators caused by electrostriction. *J Mech Phys Solids* 1994; 42 (4): 649-663.
19. Lynch CS, Yang W, Collier L, Suo ZG, McMeeking RM, Electric field induced cracking in ferroelectric ceramics. *Ferroelectrics* 1995; 166: 11-30.
20. Strobl G., *The Physics of Polymers*, Springer-Verlag, Berlin Heidelberg, 2007.
21. Li B, Chen HL, Zhou JX, et al. Polarization-modified instability and actuation mode transition. *EPL* 2011; 95 (3): 37006-12.
22. Cheng H, Torquato S. Electric-field fluctuations in random dielectric composites, *Phys Rev B* 1997; 56(13): 8060-8068.
23. Bertoldi K, Gei K. Instabilities in multilayered soft dielectrics. *J Mech Phys Solid* 2011; 59 (1): 18-42.
24. Tian L, Tevet-Deree L, deBotton G, et al. Dielectric elastomer composites. *J Mech Phys Solids* 2012; 60(1): 181-198.
25. Gent AN. A new constitutive relation for rubber. *Rubber Chem Technol* 1996; 69 (1): 59-61.
26. Mori T, Tanaka K. Average Stress in the Matrix and Average Elastic Energy of Materials with Misfitting Inclusions. *Acta Metal* 1973; 21 (5): 571-574.
27. Li B, Chen HL, Qiang JH, et al. A model for conditional polarization of the actuation enhancement of a dielectric elastomer. *Soft Matter* 2012; 8(2): 311-317.
28. Burcu E, Ravichandran G, Bhattacharya K. Large Electrostrictive Actuation of Barium Titanate Single Crystals. *J Mech Phys Solids* 2004; 52 (4): 823-846.
29. Chu B, Zhou X, Ren K, et al. A dielectric polymer with high electric energy density and fast discharge speed. *Science* 2006; 313 (5795): 334-336.
30. Keplinger C, Li T, Baumgartner R, et al. Harnessing snap-through instability in soft dielectrics to achieve giant voltage-triggered deformation, *Soft Matter* 2012; 8 (2): 285-288.
31. Huang R, Suo ZG. Electromechanical phase transition in dielectric elastomers. *Proc R Soc A* 2012; 468 (2140): 1014-1040.
32. Dang Z, Yuan J, Zha J, et al. Fundamentals, processes and applications of high-permittivity polymer-matrix composites. *Prog Mater Sci* 2012; 57 (4): 660-723.
33. Xie S, Zhu B, Wei X, et al. Polyimide/BaTiO<sub>3</sub> composites with controllable dielectric properties. *Compos A App Sci Manuf* 2005; 36 (8): 1152-1157.
34. Su J, Xu T, Zhang S, et al. An electroactive polymer-ceramic hybrid actuation system for enhanced electromechanical performance. *Appl Phys Lett* 2004; 85(6): 1045-1047.

FIGURES

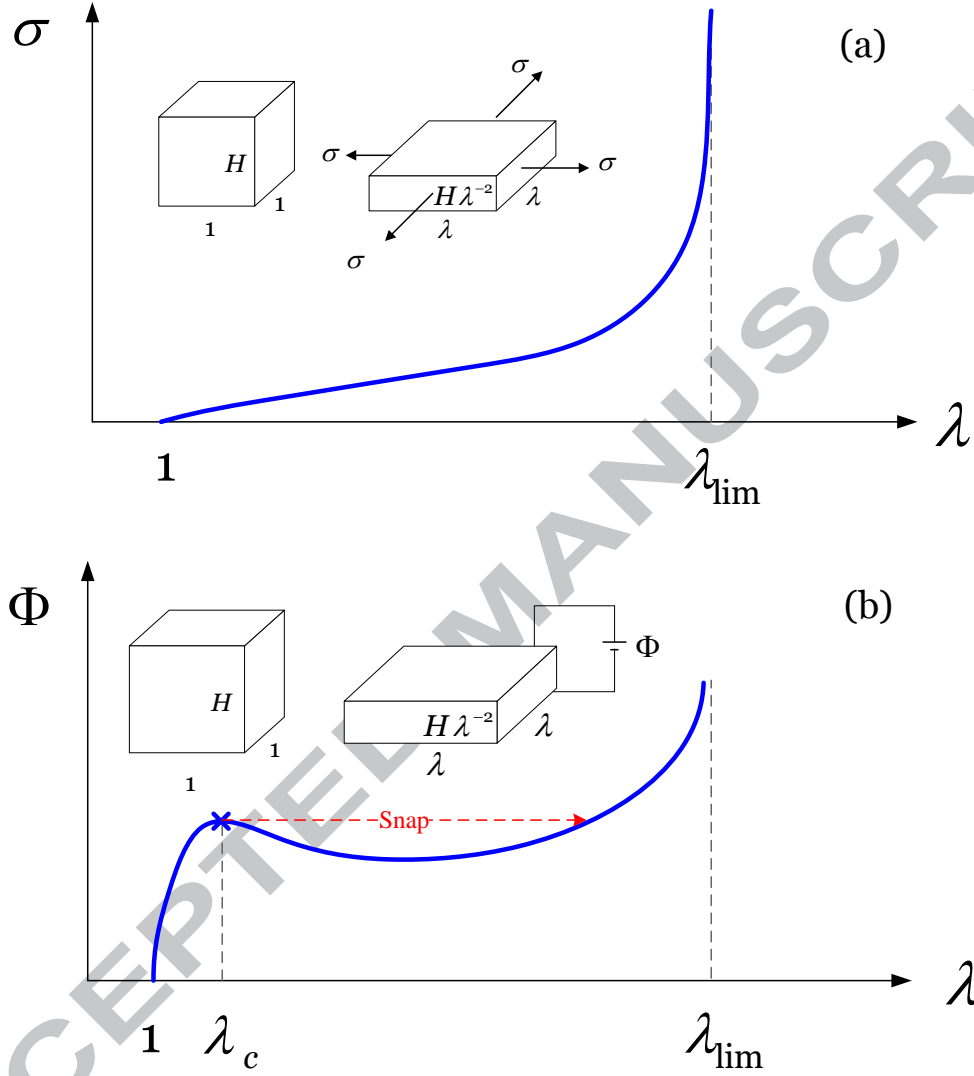
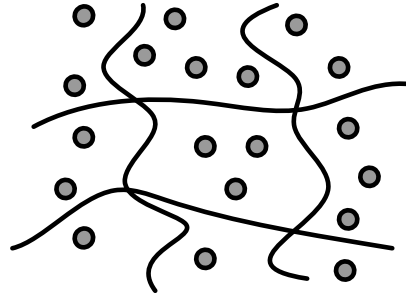
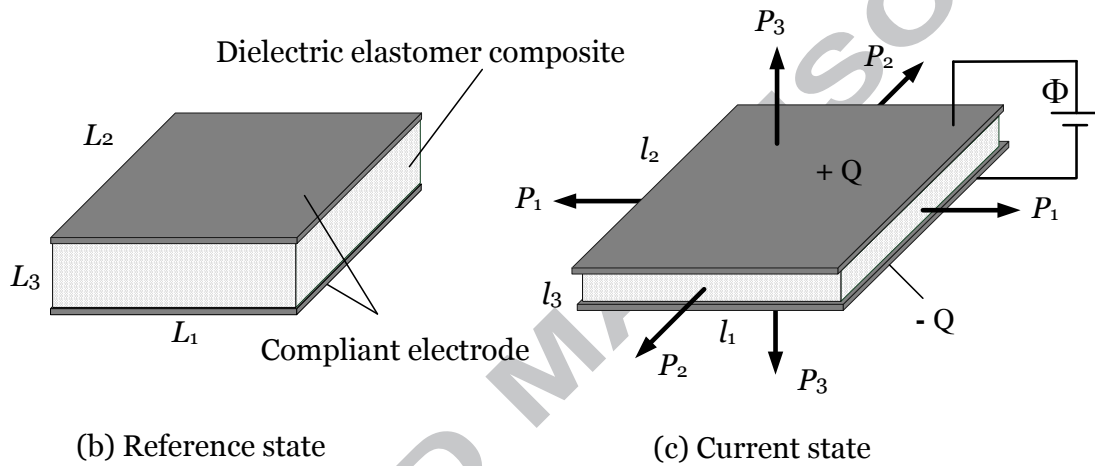


Fig. 1. (Color online) Schematic illustrations of (a) biaxial mechanical stretch curve and (b) actuation curve of the dielectric elastomer. The pull-in instability occurs at  $\lambda_c$  and the elastomer may survive by snapping through to a deformation state close to its extension limit  $\lambda_{\text{lim}}$ .



(a) Dielectric elastomer with uniform distributed fillers



(b) Reference state

(c) Current state

Fig. 2. (a) Schematic representation of a ceramic-reinforced dielectric elastomer composite. (b) Reference state of the composite with original dimensions of  $L_1$ ,  $L_2$ ,  $L_3$ . (c) By applying mechanical forces  $P$  and voltage  $\Phi$ , the thickness of the material is reduced to  $l_3$  and its area expands by  $l_1 \times l_2$  with an accumulated charge of  $Q$  at both the top and the bottom surfaces.



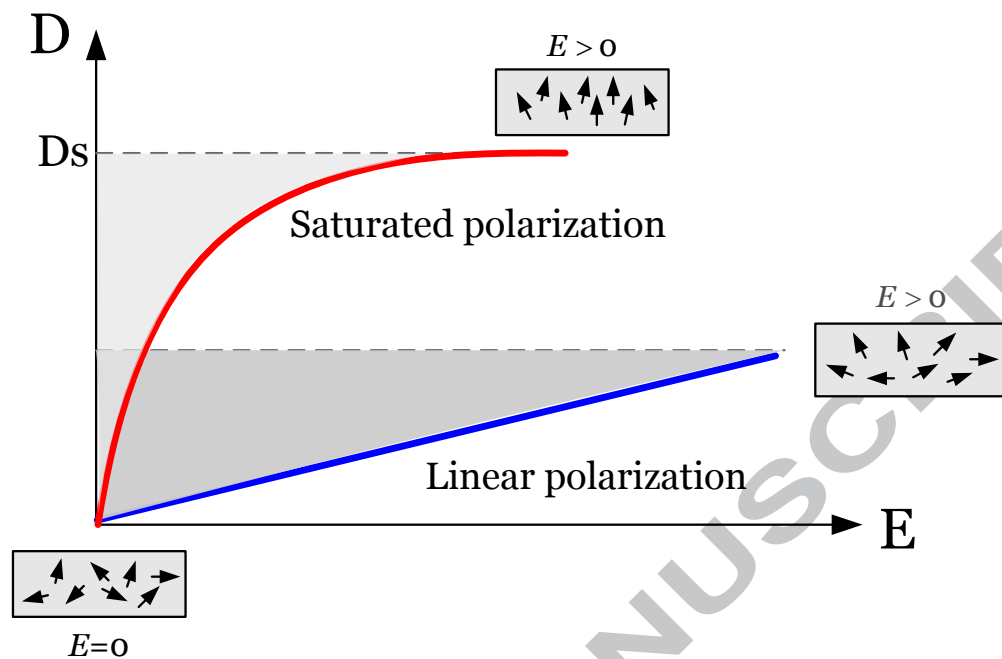


Fig. 3. (Color online) Two types of dielectric polarization: linear polarization and polarization saturation. The gray areas represent charging electrical energy.

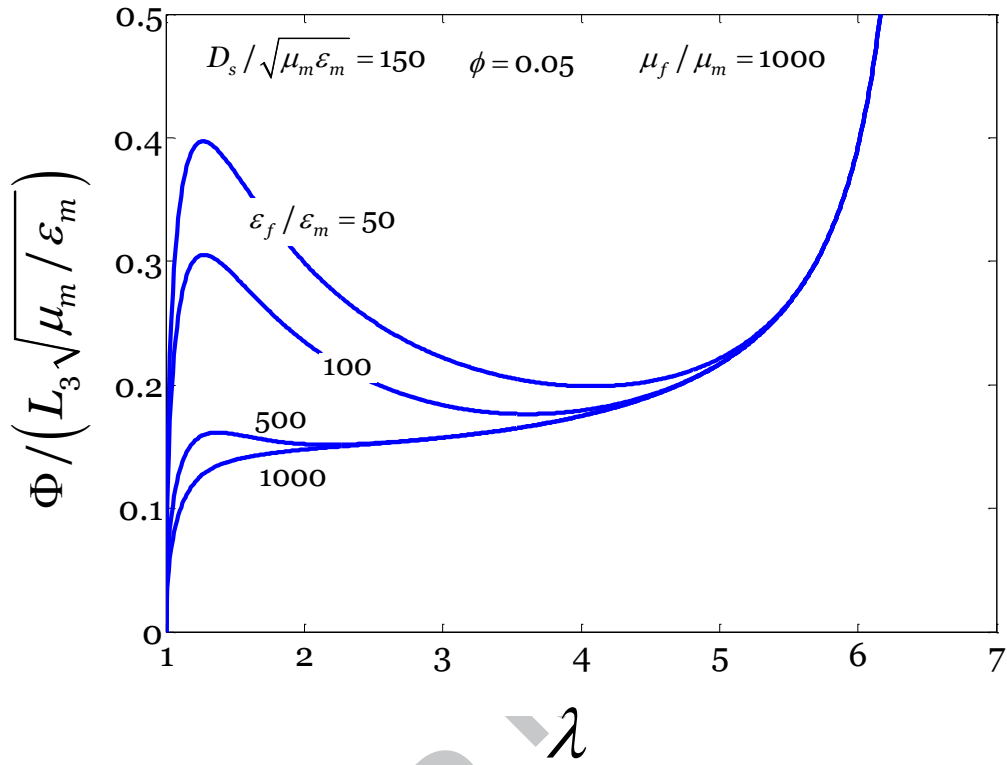


Fig. 4. Voltage-stretch curve of dielectric elastomers doped with high permittivity additives at different levels of permittivity ratio.

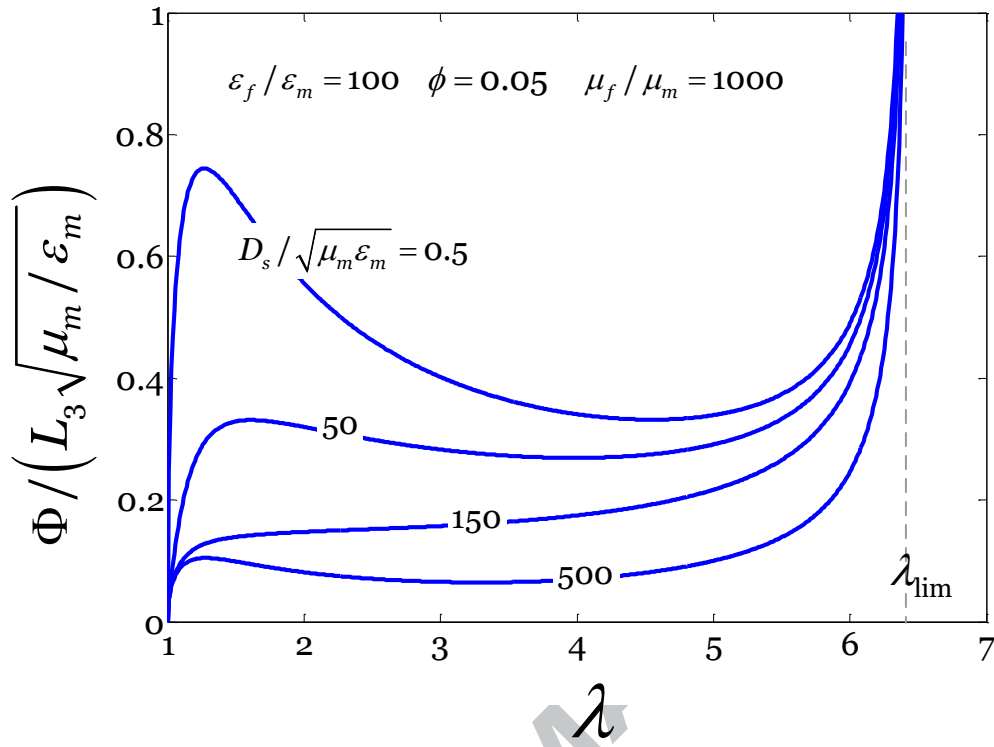


Fig. 5. Voltage-stretch curve of dielectric elastomer composites at different levels of saturated electric displacement.

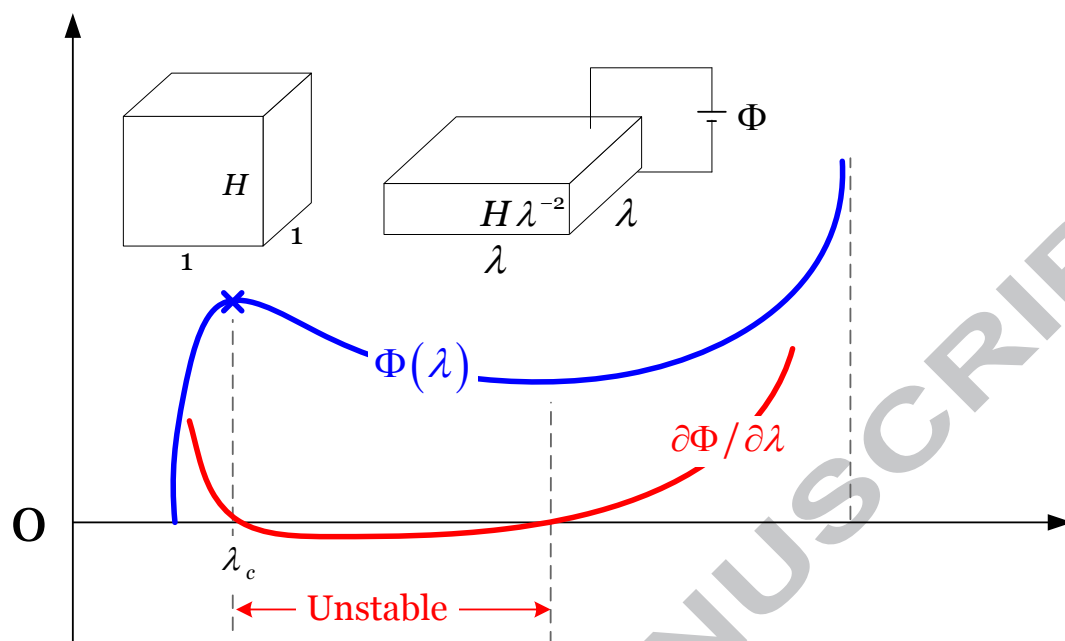


Fig. 6. (Color online) The voltage-stretch dependence curve shows two regions: stable and unstable, separated by  $\partial\Phi/\partial\lambda = 0$ .

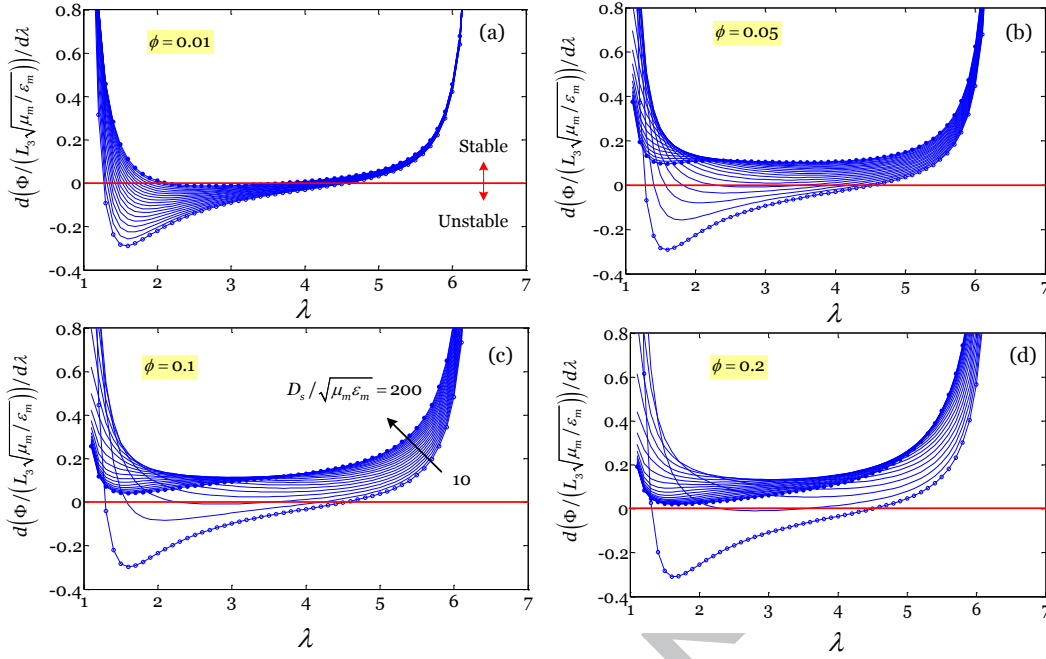


Fig. 7. (Color online) Voltage-stretch dependence of dielectric composites at different volume fractions  $\phi$  with fillers of  $\mu_f/\mu_m = 1000$  and  $\varepsilon_f/\varepsilon_m = 1000$ . From  $\circ$  to  $\bullet$ ,  $D_s/\sqrt{\mu_m\varepsilon_m}$  varies from 10 to 200, linearly.